GSK923295 as a potential antihepatocellular carcinoma agent causing delay on liver regeneration after partial hepatectomy

Jia-Cheng Tang, Ke Wu, Xing Zheng, Ming Xu, Yi Dai, Sai-Sai Wei, Xiu-Jun Cai

Key Laboratory of Endoscopic Technique Research of Zhejiang Province, Department of General Surgery, Sir Run Run Shaw Hospital, Zhejiang University, Hangzhou, Zhejiang 310016, China.

Abstract

Background: The clinical trials emerged centromere protein E inhibitor GSK923295 as a promising anticancer drug, but its function in hepatocellular carcinoma (HCC) remain needs to be fully elucidated, especially as chemotherapy after hepatectomy for liver tumors. We aimed to describe anti-HCC activities of GSK923295 and compare its antiproliferative effects on liver regeneration after partial hepatectomy (PH).

Methods: All subjects were randomized to treatment with either vehicle or GSK923295. Antitumor activity of GSK923295 was assessed by xenograft growth assays. The C57BL/6 mice were subjected to 70% PH and the proliferation was calculated by liver coefficient, further confirmed by immunohistochemistry. The proliferation and cell cycle analysis of liver cell AML12 and HCC cells LM3, HUH7, and HepG2 were investigated using the cell counting kit-8 assay and Flow Cytometry. The chromosome misalignment and segregation in AML12 cells were visualized by immunofluorescence.

Results: Treatment with GSK923295 induced antiproliferation in HCC cell lines. It also caused delay on HCC tumor growth instead of regression both in a HCC cell line xenograft model and patient-derived tumor xenograft model. With microarray analysis, CENtromere Protein E was gradually increased in mouse liver after PH. Exposure of liver cells to GSK923295 resulted in delay on a cell cycle in mitosis with a phenotype of misaligned chromosomes and chromosomes clustered. In 70% PH mouse model, GSK923295 treatment also remarkably reduced liver regeneration in later stage, in parallel with the mitotic marker phospho-histone H3 elevation.

Conclusion: The anticancer drug GSK923295 causes a significant delay on HCC tumor growth and liver regeneration after PH in later stage.

Keywords: GSK923295; Hepatocellular carcinoma; Liver regeneration; Centromere proteins E

Introduction

Hepatocellular carcinoma (HCC) is one of the most common and lethal malignant tumors, accounting for 70% to 90% of primary liver cancers.[1] Resection is currently the mainstay of treatment for patients with resectable HCC.[2,3] In some cases with advanced HCC, the 5-year overall survival rate after liver resection was reported to be over 20%,[4] suggesting that surgical resection could be effective for highly advanced HCC. However, multiple operations and anesthesia may enhance tumor implantation and growth of metastases,[5] and perioperative immunodepression may favorably affect the development of HCC. In clinic, such remnant liver tumor growth stimulation after partial hepatectomy (PH) can be reduced by treatment with chemotherapy.

Antimitotic therapies, which widely used in the clinical treatment of cancer, are effective against the abnormal proliferation of transformed cells. However, peripheral neuropathy is a major adverse effect of antimitotic drugs, as they directly inhibit the assembly of microtubule structures even in non-dividing neural cells.[6] To reduce the incidence of this side effect, a new generation of promising antimitotic drugs aiming at novel targets, especially the mitotic kinases and spindle motor proteins, has been investigated.[7] CENtromere Protein E (CENP-E) is localized at the kinetochore of chromosomes,[8] and plays an important role in the chromosome congression during prometaphase,[9] leading to the formation of stable attachment between spindle microtubules and kinetochores from prometaphase to anaphase,[10,11] in addition to the microtubule plus-end elongation.[12] To date, a total of 3 CENP-E inhibitors, including GSK923295,[13]

Access this article online

Quick Response Code:

Website: www.cmj.org

DOI: 10.1097/CM9.0000000000000053

Correspondence to: Dr. Xiu-Jun Cai, Key Laboratory of Endoscopic Technique Research of Zhejiang Province, Department of General Surgery, Sir Run Run Shaw Hospital, Zhejiang University, Hangzhou, Zhejiang 310016, China
E-Mail: Srrsh_cxj@zju.edu.com

Chinese Medical Journal 2019;132(3)

Received: 12-11-2018 **Edited by:** Yi Cui

PF-2771,[14] and CMPDA,[15] were found to exhibit antitumor activity in preclinical animal models. The clinical trials revealed GSK923295 could potentially avoid peripheral neuropathy associated with tubulin-binding chemotherapeutic agents,[16] led to emerge it as a promising anticancer drug.

Perioperative liver regeneration is one of the most important issues on radical surgery for HCC. In one hand, the growth rate of remnant liver tumor is typically more rapid than that of the liver parenchyma after surgical resection. On the other hand, hepatectomy for large or extensive liver tumors may lead to insufficient future liver remnant hypertrophy,[17] making the perioperative liver regeneration as a hot research topic on radical surgery. Basic research has elucidated that it generally takes about 8 to 10 days for a hepatoblast to mature into a hepatocyte.[18] However, the optimal time interval between neoadjuvant chemotherapy and surgery for HCC is typically 4 weeks or longer.[19] Since during hepatic regeneration, the growth rate of metastases is more rapid than that of the liver parenchyma,[20] we investigated and compared the effects of GSK923295 both on HCC and liver regeneration after PH, and demonstrated its antiproliferative activities *in vitro* and *in vivo*. This might be of great significance in improving the safety of GSK923295 as an anticancer drug for HCC.

Methods

Animal care and xenograft growth assay

All animal experiments were approved by the Committee for Animal Experiments in Zhejiang University. The mice purchased from Shanghai Laboratory Animal Co. Ltd. was administered intraperitoneally with 125 mg/kg GSK923295 in 4% *N*,*N*-dimethylacetamide (DMA)/Cremaphore (50/50) at pH 5.6 in three daily injections after PH. DMA/Cremaphore (50/50) was used as vehicle control.

Antitumor activity of GSK923295 in HCC was assessed by MHCC-LM3 cell line xenograft model[21] and patient-derived tumor xenograft (PDTX) model. Administration of GSK923295 or vehicle as described above began at days 6 to 14 when the median tumor size ranged from 80 to 100 mm^3. Each group consisted of random six nude mice (subcutaneous injection, 5×10^6 HCC cells) or four Scid mice (oxter implant, 5–10 mm^3 piece of tumor) performed xenograft growth assays. The subcutaneous tumor size was calculated and recorded every 2 day using the Vernier caliper as follows: tumor volume (mm^3) = $(L \times W^2)/2$ (L: long axis; W: short axis).

Partial hepatectomy model

About 70% PH was performed on anesthetized 8-week-old specific pathogen free female C57BL/6 mice weighing 16 to 21 g, essentially following the procedure described by Nevzorova *et al*.[22] After the mice were sacrificed, liver coefficient (liver-weight/body-weight, L/BW) was calculated immediately. For RNA analysis, liver tissues were collected at each time points after PH, immediately frozen in liquid nitrogen and stored at −80 °C until use. For immunohistochemistry analysis, tissues were fixed overnight in the formalin solution, embedded with paraffin, and sectioned.

Quantitative real-time polymerase chain reaction assays

The RNA purification was performed using RNAeasy kit (Qiagen, Germantown, USA). The polymerase chain reaction (PCR) amplification for the quantification of mRNA was performed using SsoFast EvaGreen Supermix with low ROX kit (Biorad, Hercules, USA) as previously described.[23]

Immunohistochemistry and immunofluorescence

Immunohistochemistry and immunofluorescence were performed with mouse antibodies against KI67 (Thermo, Carlsbad, USA), proliferating cell nuclear antigen (PCNA; Santa Cruz, Dallas, USA), rabbit antibody against Phospho-Histone H3 (pHH3; Cell Signaling Technology, Beverly, MA, USA) and goat antibody against albumin (ALB; Santa Cruz), the results were examined as previously described.[24]

Cell cultures and transfection

Mouse liver parenchymal cell (AML12) and three human HCC cells (HUH7, MHCC-LM3, HepG2) were bought from cell bank in Chinese Academy of Sciences. AML12 was maintained in Dulbecco's Modified Eagle Medium (DMEM)/F-12 with 1% (v/v) Insulin & Transferrin & Selenium (ITS) liquid media supplement and 40 ng/mL dexamethasone; HUH7 and LM3 were maintained in DMEM; and HepG2 was maintained in MEM.

Small interfering RNA was transiently transfected into cells with RNAi MAX reagent according to the manufacturer's instructions (Invitrogen, Carlsbad, USA).

SDS-PAGE and Western blotting analysis

Cell samples were homogenized in radioimmunoprecipitation assay buffer lysis buffer for protein extraction. Western blotting analysis was performed as previously described.[24]

Cell proliferation assay

The cell proliferation rate was determined, based on activities of dehydrogenases in cells, using the cell counting kit-8 (Dojindo, Japan).

Cell cycle analysis

After synchronize and double thymidine block (DTB), cell cycle analysis was performed as previously described.[23]

Fluorescence imaging

Cells were washed with PBS and fixed with 3.7% paraformaldehyde. Nuclei were stained by tubulin-tracker red (Beyotime, China), antibodies against CENP-E (Santa Cruz) and 4′,6-diamidino-2-phenylindole (DAPI). Samples were observed under a fluorescence microscope.

Statistical analysis

Unless otherwise stated, data are expressed as mean ± standard deviation (SD) and analyzed using the paired Student's *t*-test (GraphPad Prism 5.02; GraphPad Software, USA). A two-sided P-value < 0.05 was considered statistically significant.

Results

In vitro and in vivo anticancer activity of GSK923295 in patients with HCC

To assess the response of liver tumor to CENP-E inhibitor, we evaluated the growth inhibitory activity of GSK923295 in 3 HCC cell lines after 24, 48, and 96 hours of continuous exposure [Figure 1A]. The IC_{50} of HepG2, LM3, and HUH7 were 7.5, 5.9, and 2.9 μM, respectively. After comparing with the HCC cell proliferation rates, no correlation was observed ($P = 0.161$), suggesting that there might be unidentified and dominant factors in determining growth inhibitory effect of GSK923295. After exposure to GSK923295 for 8 hours, a large fraction of the HCC cells had proceeded into G2/M-phase. Accordingly, a significantly upregulation of the mitotic marker cyclin B1 and pHH3 was observed [Figure 1B].

To further assess antitumor activity of GSK923295 *in vivo*, we administered the inhibitor to mice bearing xenografts of the LM3 tumor cells. Compared the vehicle group,

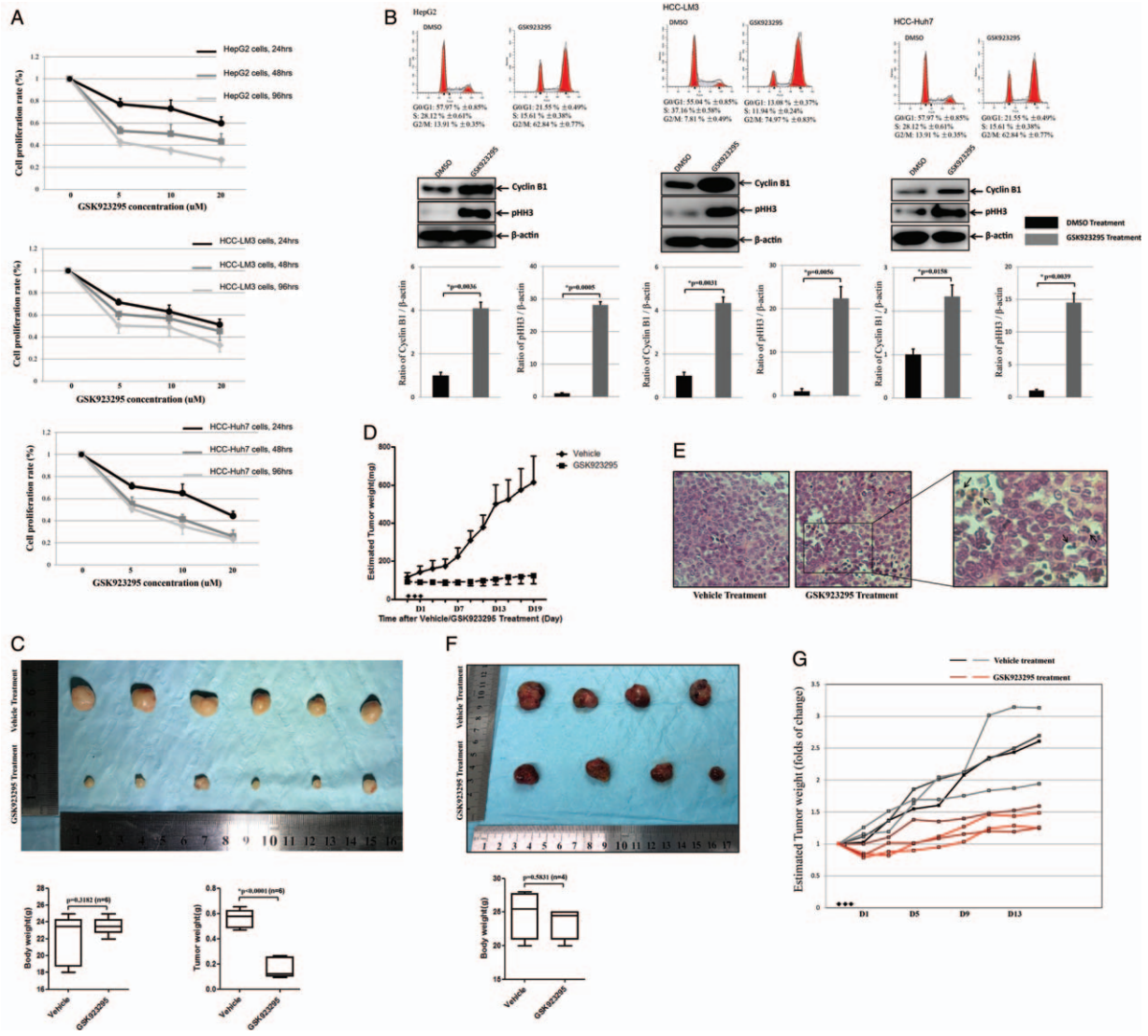

Figure 1: GSK923295 causes delay on liver tumor growth. (A) The cell proliferative activity of GSK923295-treated hepatocellular carcinoma (HCC) cells (HepG2; LM3; HUH7) for 24, 48, and 96 h were assessed by the CCK-8 assay. The *y*-axis represents the proliferation rate that calculated as a ratio to normal control (untreated cells). (B) HCC cells were arrested at the G1/S boundary by a double thymidine block (DTB). After release of DTB, HCC cells were exposure to 5 μmol/L GSK923295 for 8 h and were subjected to flow cytometry. Meanwhile, Western blotting the HCC cells treated as above was stained with cyclin B1 and pHH3. (C) After GSK923295 treatment, tumors from the LM3 were significantly smaller than those treated with vehicle at 19th day, while the total body mass showed no significant difference. (D) After 3 days of (arrowheads) GSK923295 administration, the subcutaneous tumor size was calculated and recorded every 2 days after GSK923295 or vehicle administered IP. (E) Representative photomicrograph of an H&E-stained section of LM3 tumor xenografts removed 24 h after a single injection of vehicle or GSK923295. GSK923295-induced appearance of mitotic figures (right, arrow). Scale bar: 50 μm. (F) GSK923295 treatment caused delay on tumor growth in patient-derived tumor xenograft (PDTX) model from a patient with advanced HCC. (G) After 3 days of (arrowheads) GSK923295 administration to PDTX mice, the folds of change of tumor size were diagrammatically presented.

mouse with tumor showed significantly delayed tumor volume after GSK923295 treatment [Figure 1C], with clearly increasing in the abundance of mitotic figures morphologically in tumors [Figure 1E]. The subcutaneous tumor size was calculated and recorded every 2 days, and the results demonstrated that 125 mg/kg GSK923295 caused delay on HCC tumor-growth instead of regressions [Figure 1D], because no regressions occurred in six mice treated when the study was limited on 19th day.

Furthermore, seeking to more accurately mimic the tumor environment to grow liver cancer cells, we developed a PDTX model from a 54-year-old patient with advanced HCC (Supplementary Table 1, http://links.lww.com/CM9/A7). Comparing the inhibition rate of GSK923295, it performed worse in PDTX model than that in LM3 xenograft model [Figure 1F and 1G], presumably because the former tumor microenvironment was more complicated. Taken together, these findings reflected that the administration of GSK923295 causes G2/M block in HCC xenograft models, and exhibited significant antitumor activity as well.

GSK923295 suppressed proliferation of liver cells resulted from mitotic arrest

Exposure of mouse liver cells AML12 to GSK923295 resulted in a significant inhibition on proliferation, which was in a concentration-dependent manner (Figure 2A,

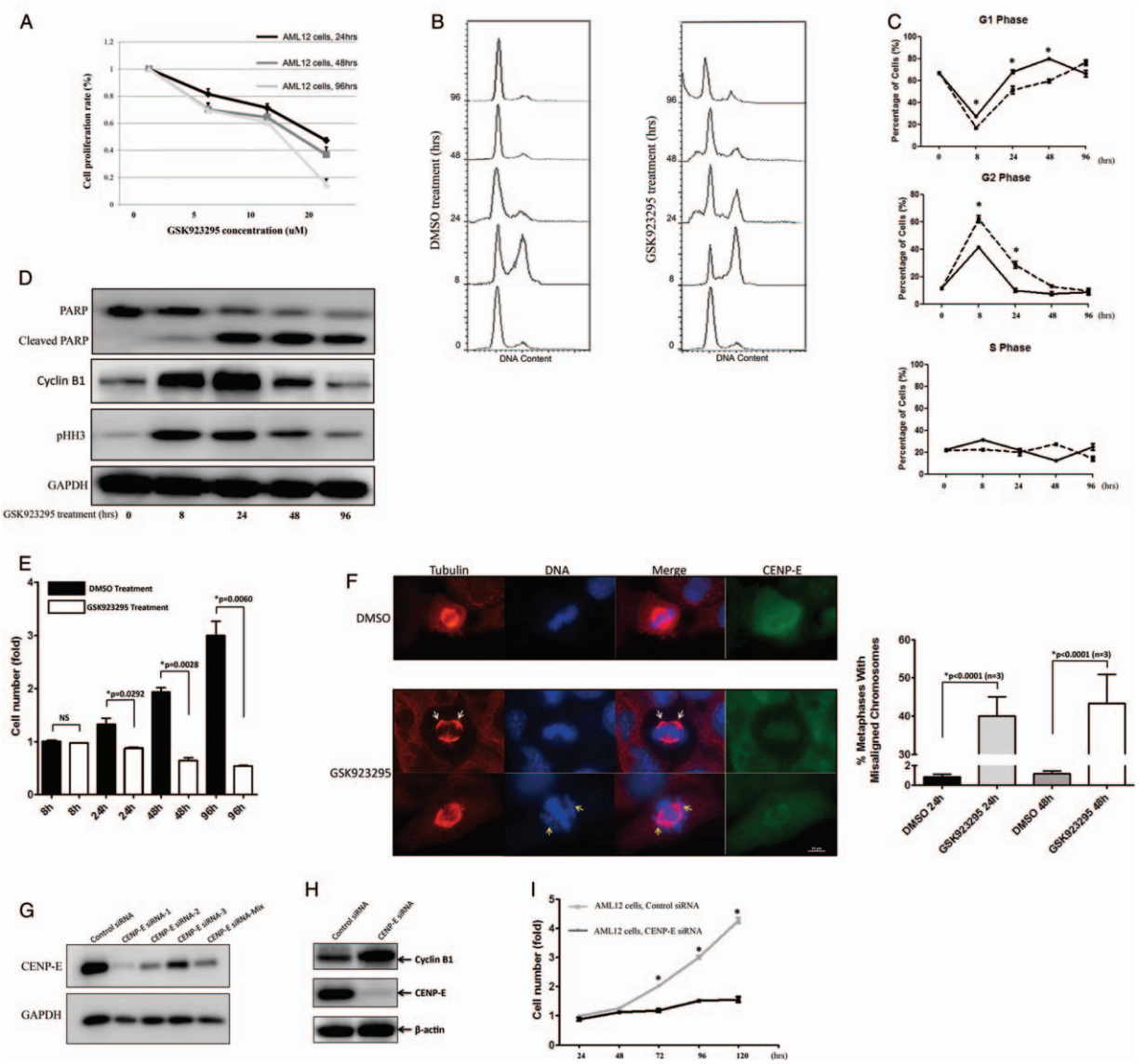

Figure 2: GSK923295 suppresses proliferation of liver cells results from mitotic arrest. (A) The proliferative activity of GSK923295-treated AML12 for 24, 48, and 96 h were assessed as described in Figure 1A. (B) After release of double thymidine block, cells were subjected to 5 μM GSK923295 for 8, 24, 48, and 96 h and under flow cytometry. (C) Quantitation of cells at different cell cycle phases after GSK923295 exposure (*$P < 0.05$, $n = 3$). (D) Western blotting the AML12 cells treated as in (B) are stained for cyclin B, and pHH3, and for cleavage of full-length poly-(ADP-Ribose) polymerase (PARP; top band) to yield a PARP fragment (bottom band), a marker of apoptosis. (E) When AML12 cells were treated with 5 μmol/L GSK923295 for 8, 24, 48, and 96 h, the relative viable cells are plotted as a histogram based on comparison to cells treated with DMSO for 8 h. (F) Metaphase in AML12 cells 24 h after GSK923295 treatment. Cells were stained with tubulin (red), DAPI (blue), and anti-CENtromere Protein E (CENP-E) antibody (green). Bar graph (right) quantitating the average mitosis duration of AML12 cells with DMSO *vs.* GSK923295 treatment or control *vs.* CENP-E knockdown, respectively. Scale bar: 10 μm. (G and H) Western blotting was performed with anti-CENP-E and GAPDH antibodies after CENP-E siRNAs were transfected into AML12 cells. Staining for cyclin B1, and CENP-E was performed as well. (G) AML12 cells were transiently transfected with negative control siRNA or CENP-E siRNA for 24, 48, 72, 96, and 120 h, the relative viable cells were measured (*$P < 0.01$, $n = 3$).

IC_{50} = 5.0 μmol/L). It also arrested the liver cells in G2/M phase [Figure 2B and 2C]. As shown in Figure 1A, cytotoxicity of GSK923295 not only was seen in HCC cancer cells, but also in healthy liver cells, particularly in cell proliferation in the liver regeneration.

Treatment of AML12 cells with GSK923295 resulted in delay in a penetrant cell cycle compared with the cells treated with DMSO (41.23% *vs*. 62.05% for DMSO and GSK923295 after 8 hours, and 10.06% *vs*. 28.64% for 24 hours in G2 phase, respectively) [Figure 2B and 2C]. Furthermore, the time-dependent accumulation of pHH3-positive cells was observed in the GSK923295-treated group. At long exposure (48 and 96 hours) to GSK923295, the percentage of cells at the G2/M phase decreased, as the cleavage of poly-(ADP-Ribose) polymerase (PARP) increased, indicating the apoptotic cell death [Figure 2D]. The viability of the AML12 cells after treatment with GSK923295 was significantly reduced as well [Figure 2E].

To investigate the influence of GSK923295 on attachment of chromosomes to spindle microtubules in liver cells, we introduced tubulin tracker to visualize the frequent mitotic abnormalities. Exposure of GSK923295 resulted in obvious defects in chromosome alignment of mitosis. In some cases, chromosomes were displaced from the metaphase plate [Figure 2F, yellow arrows] or clustered close to the spindle poles in a centrophilic position [Figure 2F, white arrows]. The percentage of mitotic cells with misaligned and/or centrophilic chromosomes increased over time, from 40% at 24 hours post-treatment to 43% at 48 hours post-treatment, whereas similar figures were never observed in more than 1% of the control samples [Figure 2F].

To validate that the GSK923295 plays its antiproliferative role in liver cells proliferation through CENP-E protein, we designed three knocking down siRNAs based on the junction site of CENP-E, and the knocking down efficiency was accordingly tested [Figure 2G], and siRNA-1 was selected for the further experiments. CENP-E siRNA transfection caused a morphologic phenotype very similar to that observed after GSK923295 treatment (data not shown), as well as the cyclin B1 expression [Figure 2H]. In addition, the growth inhibition in CENP-E knock-down cells was consistent with those obtained from GSK923295-treated AML12 cells [Figure 2I].

Consequently, GSK923295 causes failure to achieve metaphase chromosome alignment in liver cells, resulting in a roughly complete long-term mitotic arrest and apoptosis.

GSK923295 suppressed liver regeneration

To confirm the above-mentioned *in vitro* data *in vivo* findings, we developed a 70% PH mouse model [Figure 3A]. Cyclin E1,[25] Lipocalin-2,[26] and minichro-

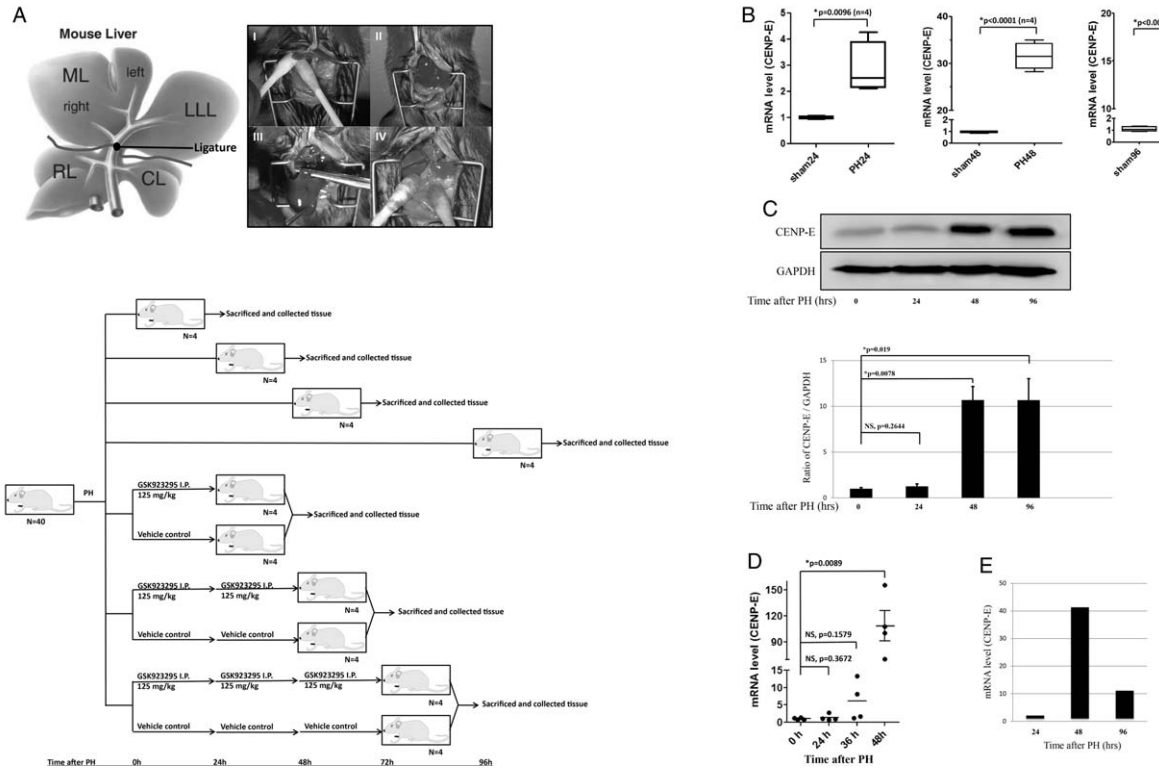

Figure 3: Expression of CENtromere Protein E (CENP-E) during mouse liver regeneration after PH. (A) Schematic representation of murine liver anatomy (Upper). I-II, Ligatured LLL, ML. III-IV, Resected LLL, ML. Diagram of procedures used to investigate the influence of GSK923295 in PH mouse model (bottom). (B) Each respectively, total RNAs were isolated from regenerative livers of PH mice and livers of sham-operated mice (24, 48, and 96 h), and the amounts of *CENP-E* mRNAs were determined as described in Materials and Methods by qPCR. (C) Western blotting analysis of CENP-E from lysates of livers at 24, 48, and 96 h after PH. (D) CENP-E expression during liver regeneration in response to PH in GEO database. The ordinates represent relative mRNA amounts and the abscissas represents the periods of time (H) after PH. (E) Expression of CENP-E in liver regeneration after PH using microarray analysis. CL: Caudate lobe; LLL: Left lateral lobe; ML: Middle lobe; qPCR: Real-time quantitative PCR detecting system; RL: Right lobe.

mosome maintenance complex component 5,[27] which were reported as upregulated genes during liver regeneration, were consistent with our results (Supplementary Table 2, http://links.lww.com/CM9/A7), indicating the liver regeneration after PH in the present study followed the same process as reported in previous studies. We also screened up- and downregulation of genes during liver regeneration at 24-, 48-, and 96-h time points using microarray analysis of mRNA expression, in which several CENP family members, including *CENP-E* (a 41.3-fold elevation at 48 hours after PH), were found and verified [Figure 3B and 3C]. Furthermore, the *CENP-E* expression in GEO database (GSE83598) followed a similar pattern with that of our results [Figure 3D and 3E]. The change of variable expression and peak stages of different respective CENP protein family members indicated that they have discriminatory functions at centromere during mitosis, and might participate in liver regeneration[28] (Supplementary Figure 1A and Supplementary Table 3, http://links.lww.com/CM9/A7).

After administration of GSK923295 or vehicle in a PH mouse model, the liver regeneration was assessed by the ratio of rest liver weight to body weight. The mean L/BW of vehicle- and GSK923295-treated group was 2.548% ± 0.199% and 2.275% ± 0.086% at 48 hours post-operation, and 3.509% ± 0.129% and 2.888% ± 0.251% at 72 hours post-operation, respectively. Compared with vehicle-treated group, the regeneration of GSK923295-treated group was remarkably reduced in later stages ($P = 0.0809$ at 48 hours, $P = 0.0319$ at 72 hours) [Figure 4A].

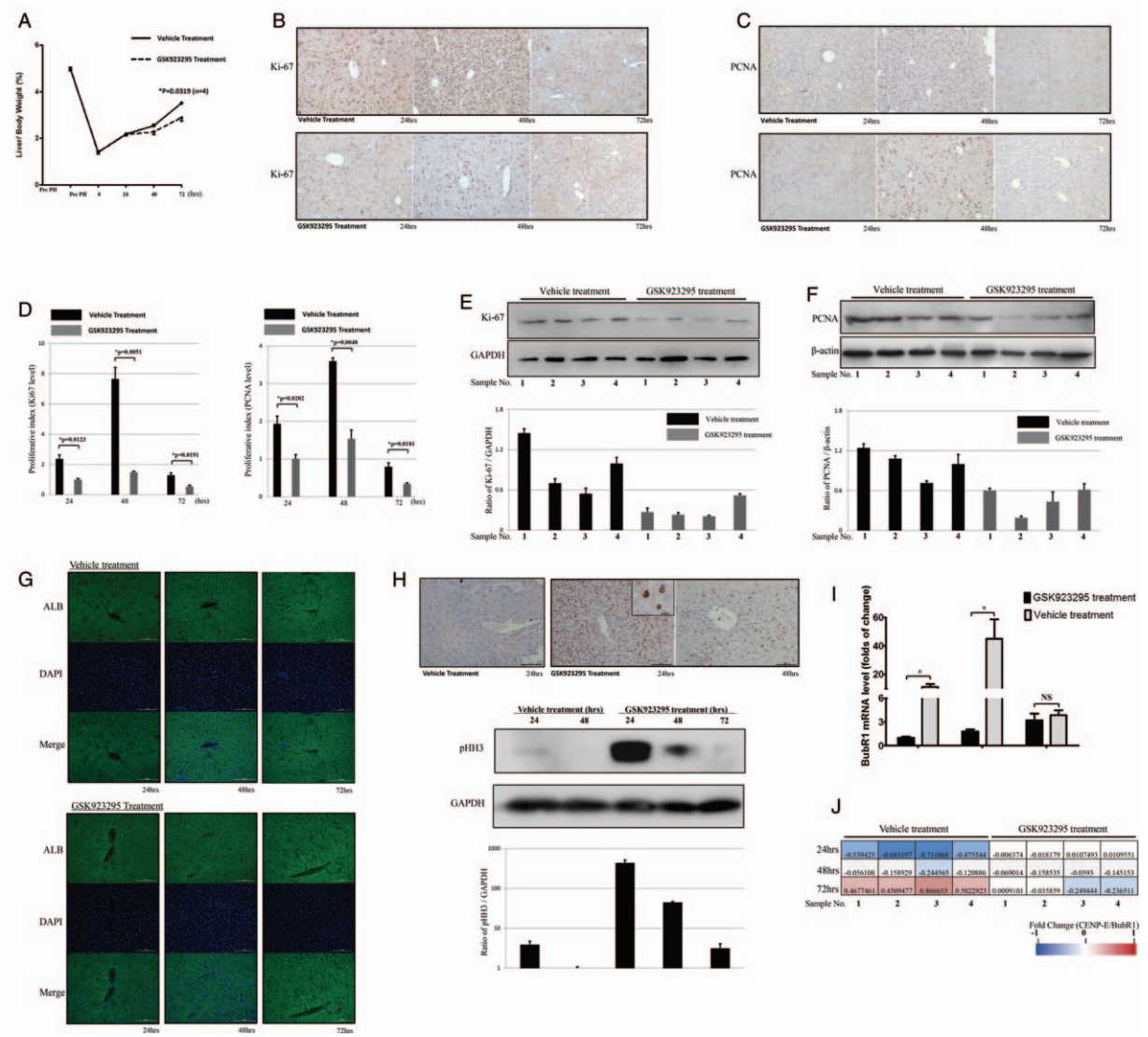

Figure 4: CENtromere Protein E (CENP-E) inhibitor GSK923295 suppresses liver regeneration. (A) Liver recovery after PH was determined by the ratio of liver/body weight ratio at indicated time points. (B and C) Representative image of Ki-67 or proliferating cell nuclear antigen (PCNA) staining by immunohistochemistry at 24, 48, and 96 h. Scale bar: 100 μm. (D) Proliferative index of different groups, which was calculated by the mean of percentage of Ki-67 or PCNA positive particle in four random visual fields (200×) stained with immunohistochemistry (IHC). (E and F) Protein level expression of Ki-67 or PCNA in each group after 48 h. (G) The protein level of ALB was measured by immunofluorescence. Scale bar:100 μm. (H) Immunohistochemistry of pHH3 in the liver sections (upper), which were verified by western blotting the corresponding tissue sample (bottom). Scale bar: 100 μm. (I) In vehicle or GSK923295-treated group, mRNA expression of *BubR1* in response to PH was determined by qPCR using the primer pairs listed in Supplementary Table 4, http://links.lww.com/CM9/A7. $^{*}P < 0.01$. (J) The relationship between CENP-E and BubR1 in vehicle or GSK923295-treated groups was calculated by the ratio of *CENP-E/BubR1* mRNA levels. The $\log_{10}$ of the ratio was filled in the form with color key.

The variation of regenerative response was further confirmed by the staining of Ki-67 [Figure 4B] and PCNA [Figure 4C] as classical markers for cell proliferation. The staining scores were calculated as the proliferation index of the two groups and then compared [Figure 4D]. Both in Ki-67 group and PCNA group, the proliferation index significantly increased at 48 hours after operation. However, the vehicle-treated group was more active than that of the GSK923295 treated in the whole course. The expressions of Ki-67 and PCNA in each group with all 4 samples after 48 hours were detected by Western blotting [Figure 4E and 4F] as well. The level of pHH3 increased to a peak at 24 hours after administration, then rapidly decreased at 48 hours and was minimal at 72 hours. Accordingly, immunohistochemistry of the liver sections showed the accumulation of pHH3-positive cells 24 hours after the administration of GSK923295 [Figure 4H]. Meanwhile, the expression of ALB was measured to evaluate the hepatic function, and no intergroup discrepancy was clarified [Figure 4G].

Since CENP-E interacts with BubR1 kinase and modulating its activities,[29] we investigate the influence of GSK923295 on the expression of BubR1 in liver regeneration in PH mouse. BubR1 was significantly upregulated 48 hours after operation in vehicle-treated group, while in GSK923295-treated group, the expression was low and delayed, similar to (but less than) that observed in sham-operated group [Figure 4I]. Upon further investigation, we compared the expression status of CENP-E and BubR1 in all samples at each time point, the linear correlation coefficient was 0.7057 for vehicle group and 0.6678 for GSK923295 group, respectively [Figure 4J]. These findings show CENP-E might be essential for BubR1 to function in liver regeneration.

Discussion

To our best knowledge, it is the rare report to elucidate GSK923295 function as a potential anti-HCC agent, which markedly suppressed liver regeneration in PH mouse model. GSK923295 is a 1st-in-class, specific, and allosteric inhibitor of CENP-E function. In a phase I clinical trial, as the next generation of mitotic inhibitor, GSK923295 showed low incidence of myelosuppression and neuropathy among patients with refractory solid tumors,[16] necessitating that further studies are required to analyze its antiproliferative capability as chemotherapeutic agents.

In this study, we assessed the growth inhibitory activity of GSK923295 in HCC. GSK923295 treatment led to G2/M arrest in HCC cells, and *in vivo* assay showed a significant antiproliferative activity against LM3 xenografts and PDTX model. Similar to our results, GSK923295 resulted in mitotic arrest and colon tumor regression in xenograft models.[13] However, GSK923295 contained various antitumor activities in different cancer cell xenografts. For instance, it produced partial or even complete regressions at the 125 mg/kg dose against Colo205 xenografts, while such robust antitumor activity took the edge off in HCC. Our PDTX model also showed that such dose of GSK923295 only caused delay on tumor growth without regression (consistent with the higher IC50 for HCC cells). Since the maximal-tolerated dose in mice is over 500 mg/kg,[13] a follow-up research should set higher dose of GSK923295 for HCC cells *in vivo*.

According to our results, GSK923295 showed the same level of inhibition to liver cells, when it was compared with HCC cells *in vitro*. Furthermore, an elaborate detection of hepatic function in PH mouse was performed as well. The aspartate aminotransferase and alanine aminotransferase levels gradually increased 24 hours after PH, decreased by over 50% after 48 hours, and reached normal level after 96 hours. Total bilirubin increased to high levels 24 hours after PH, which showed a slight decrease after 48 hours, and again reached normal level after 96 hours. Compared with the GSK923295 treatment group, no significant differences were found (data not shown). Meanwhile, the expression of ALB showed that there was no discrepancy, which revealed that the functional maturity in the process of liver regeneration after PH is very complicated to be determined by merely several detection indexes. Further studies are required to evaluate hepatic function and liver tumor response to GSK923295 using a sufficiently large sample size, and optimize the treatment schedules of resectable HCC, especially for hepatectomy for large or extensive liver tumors, which usually lead to insufficient future liver remnant hypertrophy.

Since previous studies have revealed that *CENP-E* mRNA expression does not correlate with sensitivity to the CENP-E inhibitor,[13,15]*CENP-E* expression might not be a feasible biomarker for predicting tumors that are sensitive to the GSK923295. In this studies, the inhibitory effects of centromere by GSK923295 were determined in cells with pole-proximal misaligned chromosomes. In parallel with the mitotic aberration, we also observed the mitotic marker pHH3 elevated *in vitro* and *in vivo*, while its level fall rapidly after GSK923295 treatment. Considering that BubR1 kinase activity associates with histone H3 phosphorylation[30] and is directly stimulated by CENP-E,[29] pHH3 could potentially be used as an efficient marker for GSK923295 to indirectly monitor CENP-E motor activity. Further preclinical studies in HCC models might be required to develop the utility of pHH3 as a biomarker for GSK923295.

In summary, we report that GSK923295 functions antitumor activity in HCC cells and leads to a significant delay in liver regeneration after PH. We also compare antiproliferative effects of GSK923295 both on HCC and liver regeneration after PH, in which no significant discrepancy in level of inhibition is observed according to our results.

Funding

This study was supported by the grants from the National Natural Science Foundation of China (No. 81602623) and Zhejiang Provincial Natural Science Foundation of China (No. LY19H200004).

Conflicts of interest

None.

References

1. Torre LA, Bray F, Siegel RL, Ferlay J, Lortet-Tieulent J, Jemal A. Global cancer statistics, 2012. CA Cancer J Clin 2015;65:87–108. doi: 10.3322/caac.21262.
2. Forner A, Llovet JM, Bruix J. Hepatocellular carcinoma. Lancet 2012;379:1245–1255. doi: 10.1016/S0140-6736(11)61347-0.
3. Sapisochin G, Goldaracena N, Laurence JM, Dib M, Barbas A, Ghanekar A, *et al*. The extended Toronto criteria for liver transplantation in patients with hepatocellular carcinoma: a prospective validation study. Hepatology 2016;64:2077–2088. doi: 10.1002/hep.28643.
4. Ban D, Shimada K, Yamamoto Y, Nara S, Esaki M, Sakamoto Y, *et al*. Efficacy of a hepatectomy and a tumor thrombectomy for hepatocellular carcinoma with tumor thrombus extending to the main portal vein. J Gastrointest Surg 2009;13:1921–1928. doi: 10.1007/s11605-009-0998-0.
5. Weese JL, Ottery FD, Emoto SE. Do operations facilitate tumor growth? An experimental model in rats. Surgery 1986;100:273–277.
6. Jordan MA, Wilson L. Microtubules as a target for anticancer drugs. Nat Rev Cancer 2004;4:253–265. doi: 10.1038/nrc1317.
7. Chan KS, Koh CG, Li HY. Mitosis-targeted anti-cancer therapies: where they stand. Cell Death Dis 2012;3:e411. doi: 10.1038/cddis.2012.148.
8. Yen TJ, Li G, Schaar BT, Szilak I, Cleveland DW. CENP-E is a putative kinetochore motor that accumulates just before mitosis. Nature 1992;359:536–539. doi: 10.1038/359536a0.
9. Wood KW, Sakowicz R, Goldstein LS, Cleveland DW. CENP-E is a plus end-directed kinetochore motor required for metaphase chromosome alignment. Cell 1997;91:357–366. doi.org/10.1016/s0092-8674(00)80419-5.
10. Gudimchuk N, Vitre B, Kim Y, Kiyatkin A, Cleveland DW, Ataullakhanov FI, *et al*. Kinetochore kinesin CENP-E is a processive bi-directional tracker of dynamic microtubule tips. Nat Cell Biol 2013;15:1079–1088. doi: 10.1038/ncb2831.
11. Vitre B, Gudimchuk N, Borda R, Kim Y, Heuser JE, Cleveland DW, *et al*. Kinetochore-microtubule attachment throughout mitosis potentiated by the elongated stalk of the kinetochore kinesin CENP-E. Mol Biol Cell 2014;25:2272–2281. doi: 10.1091/mbc.E14-01-0698.
12. Sardar HS, Luczak VG, Lopez MM, Lister BC, Gilbert SP. Mitotic kinesin CENP-E promotes microtubule plus-end elongation. Curr Biol 2010;20:1648–1653. doi: 10.1016/j.cub.2010.08.001.
13. Wood KW, Lad L, Luo L, Qian X, Knight SD, Nevins N, *et al*. Antitumor activity of an allosteric inhibitor of centromere-associated protein-E. Proc Natl Acad Sci U S A 2010;107:5839–5844. doi: 10.1073/pnas.0915068107.
14. Kung PP, Martinez R, Zhu Z, Zager M, Blasina A, Rymer I, *et al*. Chemogenetic evaluation of the mitotic kinesin CENP-E reveals a critical role in triple-negative breast cancer. Mol Cancer Ther 2014;13:2104–2115. doi: 10.1158/1535-7163.MCT-14-0083-T.
15. Ohashi A, Ohori M, Iwai K, Nambu T, Miyamoto M, Kawamoto T, *et al*. A novel time-dependent CENP-E inhibitor with potent antitumor activity. PLoS One 2015;10:e144675. doi: 10.1371/journal.pone.0144675.
16. Chung V, Heath EI, Schelman WR, Johnson BM, Kirby LC, Lynch KM, *et al*. First-time-in-human study of GSK923295, a novel antimitotic inhibitor of centromere-associated protein E (CENP-E), in patients with refractory cancer. Cancer Chemother Pharmacol 2012;69:733–741. doi: 10.1007/s00280-011-1756-z.
17. Inoue Y, Tanaka R, Fujii K, Kawaguchi N, Ishii M, Masubuchi S, *et al*. Surgical outcome and hepatic regeneration after hepatic resection for hepatocellular carcinoma in elderly patients. Dig Surg 2018;1–13. doi: 10.1159/000488327.
18. Chaudhari P, Tian L, Deshmukh A, Jang YY. Expression kinetics of hepatic progenitor markers in cellular models of human liver development recapitulating hepatocyte and biliary cell fate commitment. Exp Biol Med (Maywood) 2016;241:1653–1662. doi: 10.1177/1535370216657901.
19. Lai EC, Lo CM, Fan ST, Liu CL, Wong J. Postoperative adjuvant chemotherapy after curative resection of hepatocellular carcinoma: a randomized controlled trial. Arch Surg 1998;133:183–188. doi.org/10.1001/archsurg.133.2.183.
20. Elias D, De Baere T, Roche A, Mducreux , Leclere J, Lasser P. During liver regeneration following right portal embolization the growth rate of liver metastases is more rapid than that of the liver parenchyma. Br J Surg 1999;86:784–788. doi: 10.1046/j.1365-2168.1999.01154.x.
21. Zheng L, Xu M, Xu J, Wu K, Fang Q, Liang Y, *et al*. ELF3 promotes epithelial-mesenchymal transition by protecting ZEB1 from miR-141-3p-mediated silencing in hepatocellular carcinoma. Cell Death Dis 2018;9:387. doi: 10.1038/s41419-018-0399-y.
22. Nevzorova YA, Tolba R, Trautwein C, Liedtke C. Partial hepatectomy in mice. Lab Anim 2015;49:81–88. doi: 10.1177/0023677215572000.
23. Liang X, Tang J, Liang Y, Jin R, Cai X. Suppression of autophagy by chloroquine sensitizes 5-fluorouracil-mediated cell death in gallbladder carcinoma cells. Cell Biosci 2014;4:10. doi: 10.1186/2045-3701-4-10.
24. Tang JC, Liu JH, Liu XL, Liang X, Cai XJ. Effect of fibulin-5 on adhesion, migration and invasion of hepatocellular carcinoma cells via an integrin-dependent mechanism. World J Gastroenterol 2015;21:11127–11140. doi: 10.3748/wjg.v21.i39.11127.
25. Stratton SA, Barton MC. Hierarchy of a regenerative cell cycle: cyclin E1 multitasks. Hepatology 2014;59:370–371. doi: 10.1002/hep.26658.
26. Kienzl-Wagner K, Moschen AR, Geiger S, Bichler A, Aigner F, Brandacher G, *et al*. The role of lipocalin-2 in liver regeneration. Liver Int 2015;35:1195–1202. doi: 10.1111/liv.12634.
27. Zhou Y, Xu J, Liu Y, Li J, Chang C, Xu C. Rat hepatocytes weighted gene co-expression network analysis identifies specific modules and hub genes related to liver regeneration after partial hepatectomy. PLoS One 2014;9:e94868. doi: 10.1371/journal.pone.0094868.
28. Glynn M, Kaczmarczyk A, Prendergast L, Quinn N, Sullivan KF. Centromeres: assembling and propagating epigenetic function. Subcell Biochem 2010;50:223–249. doi: 10.1007/978-90-481-3471-7_12.
29. Mao Y, Abrieu A, Cleveland DW. Activating and silencing the mitotic checkpoint through CENP-E-dependent activation/inactivation of BubR1. Cell 2003;114:87–98. doi.org/10.1016/s0092-8674(03)00475-6.
30. Ditchfield C, Johnson VL, Tighe A, Ellston R, Haworth C, Johnson T, *et al*. Aurora B couples chromosome alignment with anaphase by targeting BubR1, Mad2, and Cenp-E to kinetochores. J Cell Biol 2003;161:267–280. doi: 10.1083/jcb.200208091.

How to cite this article: Tang JC, Wu K, Zheng X, Xu M, Dai Y, Wei SS, Cai XJ. GSK923295 as a potential antihepatocellular carcinoma agent causing delay on liver regeneration after partial hepatectomy. Chin Med J 2019;132:311–318. doi: 10.1097/CM9.0000000000000053